Article

Maximising Distribution Grid Utilisation by Optimising E-Car Charging Using Smart Meter Gateway Data

André Ulrich *, Sergej Baum, Ingo Stadler, Christian Hotz and Eberhard Waffenschmidt

Cologne Institute for Renewable Energies (CIRE), TH Köln, 51519 Cologne, Germany
* Correspondence: andre.ulrich@th-koeln.de

Abstract: The transition towards climate neutrality will result in an increase in electrical vehicles, as well as other electric loads, leading to higher loads on electrical distribution grids. This paper presents an optimisation algorithm that enables the integration of more loads into distribution grid infrastructure using information from smart meters and/or smart meter gateways. To achieve this, a mathematical programming formulation was developed and implemented. The algorithm determines the optimal charging schedule for all electric vehicles connected to the distribution grid, taking into account various criteria to avoid violating physical grid limitations and ensuring non-discriminatory charging of all electric vehicles on the grid while also optimising grid operation. Additionally, the expandability of the infrastructure and fail-safe operation are considered through the decentralisation of all components. Various scenarios are modelled and evaluated in a simulation environment. The results demonstrate that the developed optimisation algorithm allows for higher transformer loads compared to a P(U) control approach, without causing grid overload as observed in scenarios without optimisation or P(U) control.

Keywords: electric vehicle; optimisation; linear programming; smart meter gateway; grid load

1. Introduction

The Paris Climate Agreement has set targets for effective action on common climate policies to limit the global temperature increase to well below 2 °C within the current century. Progress has recently been made in climate policy, particularly in Europe and Asia. For example, China, the world's largest emitter of CO_2, has announced its intention to achieve climate neutrality by 2060. Neighboring countries such as South Korea and Japan aim to achieve this goal even earlier—by 2050. The EU also plans to follow suit by reducing greenhouse gas emissions by 55% by 2030 compared to 1990 levels, becoming completely climate-neutral by 2050.

One potential solution for reducing CO_2 emissions is the electrification of freight and passenger transport [1]. Registrations of electric vehicles (EVs) and vans in Europe significantly increased in 2020, reaching nearly 1,325,000 units, up from 550,000 units in 2019. This represents a 3.5% increase, accounting for 11% of total new registrations in just one year. Furthermore, the share of electric vans increased from 1.4% of total new registrations in 2019 to 2.2% in 2020. Battery electric vehicles, rather than plug-in hybrids, accounted for the majority of electric van and passenger car registrations in 2020 [2]. While Norway has the largest share of EV registrations among European countries, Germany leads the European market for plug-in electric car sales. In Norway, which has a population of around 5.4 million people, every second newly registered car is a battery electric vehicle [3].

While electric vehicles have a positive impact on the climate, the integration of a large number of EVs into the public grid can have some disadvantages, such as the potential overloading of electricity grids during the charging process. This paper presents a possible solution to this problem, along with a control algorithm for charging stations, developed

as part of the PROGRESSUS project. Based on the grid topology, household loads, estimated driving performance, state of charge (SOC), and departure time, the new algorithm determines an optimal charging schedule for all charging stations. The aim is to achieve non-discriminatory charging of all EVs in the network, taking into account various influencing factors while ensuring optimal network operation. Additionally, attention was given to the expandability of the infrastructure and fail safety through the decentralisation of all components.

2. State of the Art

Several optimisation solutions in the field of power supply and power flow optimisation have been proposed and investigated. Most of previous studies have focused on technical and economic issues, with the aim of minimising supply costs while also considering ecological aspects. Different algorithm designs and methods have been investigated and improved. In [4], an energy management model was introduced to determine the optimal operation strategies with maximum profit for a microgrid system. The simulation environment includes energy storage, photovoltaic, and wind power systems. In this study, the investment demand in storage capacities with growing electricity demand was investigated.

Mixed-integer optimisation algorithms were also used in [5] for the purpose of technical and economic optimisation of power supply in microgrids. The integration of a large number of PV systems into the distribution network and the associated problems were studied by Bhatt et al. [6]. The focus was on reducing harmonics, voltage fluctuations, poor power factors, and power losses. For optimisation purposes, a "novel population-based algorithm" [7] was used in [6].

In [8], a new optimisation approach based on a hybrid algorithm consisting of biogeography-based optimisation with an adaptive mutation scheme and the concept of predator–prey optimisation was presented to achieve optimal energy flow. The proposed method was tested on an IEEE 30-bus test system, with the main objectives of reducing losses in the network, improving the voltage profile, and increasing voltage stability. Comparison of the results with other approaches demonstrates the effectiveness and robustness of the proposed optimisation method.

Ehab et al. [9] proposed a new version of the JAYA algorithm to solve the problem of optimal power flow while considering objectives such as minimum fuel cost, minimum emissions, least transmission losses, and improved voltage profile. The application of the new algorithm resulted in better results in terms of saving CO_2 emissions and fuel cost compared to other methods. Other algorithms such as particle swarm optimisation [10] and artificial bee colony [11] algorithms have also been applied to achieve power flow optimisation.

Numerous studies have investigated the integration of a large number of EVs into public grids. In [12], a centralised control mechanism was investigated to integrate EVs while maintaining stability criteria. However, this control mechanism does not consider predictions such as EVs mileage, driving distance, etc.; therefore, load shifting or time-shifted charging may not be possible.

In comparison to the work of Peças Lopes et al. [12], Sortomme et al. [13] investigated the influence of plug-in hybrid vehicles on medium-voltage grids. Three charging algorithms were developed and investigated by Ahn et al. [14], who proposed a two-level distributed charging algorithm for EVs that provides both load shifting and frequency control. Load shifting was achieved by coordinating EV charging and electricity generation, resulting in reduced carbon dioxide emissions and electricity generation costs. A linear problem was formulated for the optimisation algorithm.

Decentralised solutions for EV integration were proposed and investigated in [15,16]. In contrast to other studies, the focus of power flow optimisation in [17] was not on CO_2 minimisation or cost reduction for energy generation. Instead, the study reported in [17] addressed the control of residential EV chargers connected to a low-voltage power grid

with a tree-like operational structure. The available capacity of the power grid, measured by distribution-level phasor measurement units, was divided in a proportionally fair manner among connected EVs, considering their demands and self-declared deadlines. This approach is closest to that investigated in our study. However, the proposed optimisation method requires measuring units to be installed at every node in the considered grid, as pointed out by Zishan et al. [17].

As of now, there is no available solution that can coordinate EV charging based on only a limited number of measurement points. In other studies, measurements at every node are typically required to accurately determine the state of the grid, and the topology of the grid needs to be known in advance. In [17], although a "fair" distribution of charging power was mentioned, there were no constraints to ensure that lines were not overloaded and that node voltages did not drop too far.

In our study, we eliminated these problems. Using only a limited number of measurements from smart meter gateways, we were able to determine the grid topology and grid state. Our optimisation algorithm provides the maximum charging power at the charging stations, as well as optimal utilisation of the electric power grid. Additionally, we offer different implementations of "fair" charging.

3. Materials and Methods

As outlined in Section 1, the objective is to maximise the utilisation of the distribution grid, enabling it to operate at its capacity limits. However, it is also crucial to ensure that no criteria for grid overloading are breached. The criteria for grid overload, as considered in this study, are summarised in Table 1.

Table 1. Observed criteria for grid overloading.

Observed Criterion	Unit	Allowed Limit
Transformer load	%	≤ 100
Line load	%	≤ 100
Node voltage	$\% U_{\text{nominal}}$	$\leq \pm 6$ [18]

In addition, it is important to take into account customer requirements. Whenever feasible, all customer requests should be accommodated. To achieve this, an optimisation algorithm was developed using Python programming language and the Pyomo optimisation framework [19]. The GNU Linear Programming Kit (glpk) [20] is employed as the solver. The developed algorithm is based on linear programming techniques.

Linear programming requires certain input parameters to be available, as discussed in Section 3.2. However, in some cases, all of these input data may not be be readily available. For instance, measurements from smart meter gateways (SMGs) at grid nodes, such as charging boxes, may be the only available data. To address this limitation, other algorithms, such as grid topology estimation (GTE) and grid state estimation (GSE), can be employed to reconstruct the required input data from the available measurements. These techniques are described in [21], although they are not specifically discussed in this paper. However, the findings from GTE and GSE are applied in the proposed grid line optimiser (GLO) system, as depicted in Figure 1, to determine the optimal charging power and utilisation of the electric power grid.
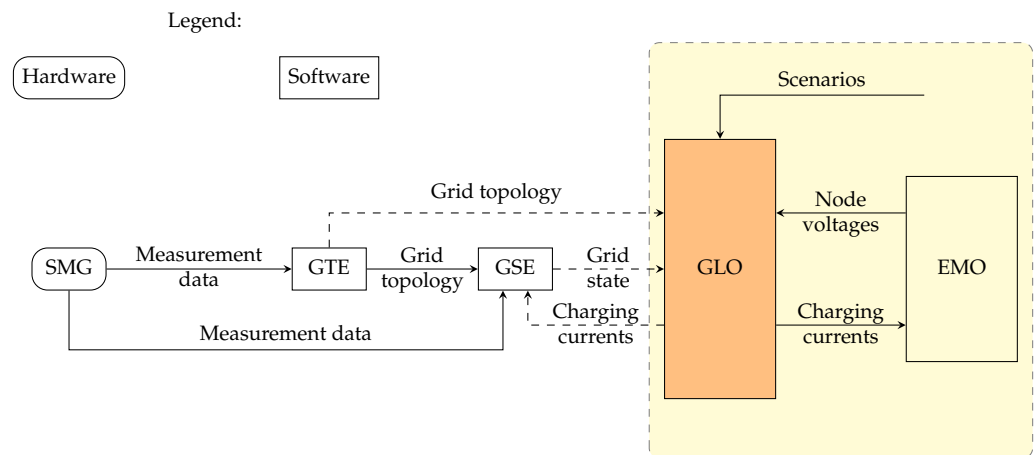
Figure 1. System structure (SMG: smart meter gateway; GTE: grid topology estimation; GSE: grid state estimation; GLO: grid line optimiser; EMO: simulation environment).

3.1. The Principle of the Algorithm

Linear programming determines an optimal charging schedule for all attached charging EVs according to the following input parameters:

Household load profiles: Predicted household profiles are needed so that the optimiser can shift the EV chargings in order to react to fluctuating household loads;

Grid topology: Knowledge of the grid topology, such as line impedances and lengths, transformer nominal power, and the positions of the charging stations, is required for correct calculations of node voltages and currents on the lines;

Customer requests: Desired target SOCs and times, as well as start SOCs and times, are required for optimisation to prioritise which EVs to charge;

Settings for time: The optimiser requires time settings to know which horizon (e.g., 24 h) to predict and at what resolution (e.g., 15 min).

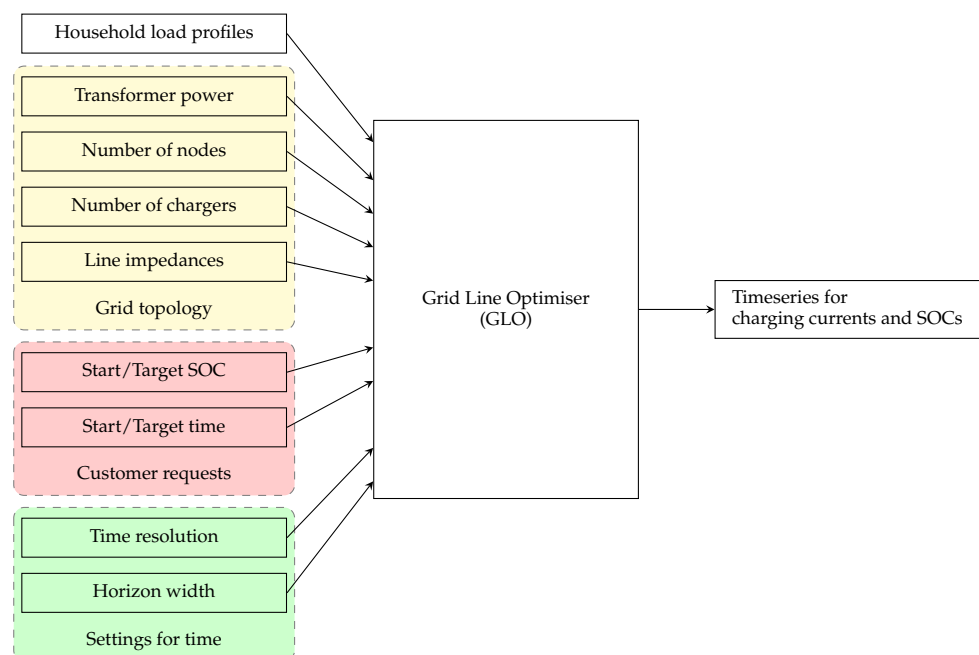All the required input parameters, as well as the output of the optimisation, are shown in Figure 2.

Figure 2. Inputs and outputs of the optimisation algorithm (GLO).

In Figure 3, the "considered horizon/resolution" and the information on the number of nodes and chargers from the "grid topology" are used to construct sets for indexing. These sets are used to construct parameters in the optimisation model. The household load profiles are also directly used as parameters in the optimisation model. The "customer requests" are used to determine variable upper and lower bounds in the optimisation model. This information is used to set constraints and boundaries for the optimisation process, ensuring that the solution adheres to the specific requirements and requests of the customers.
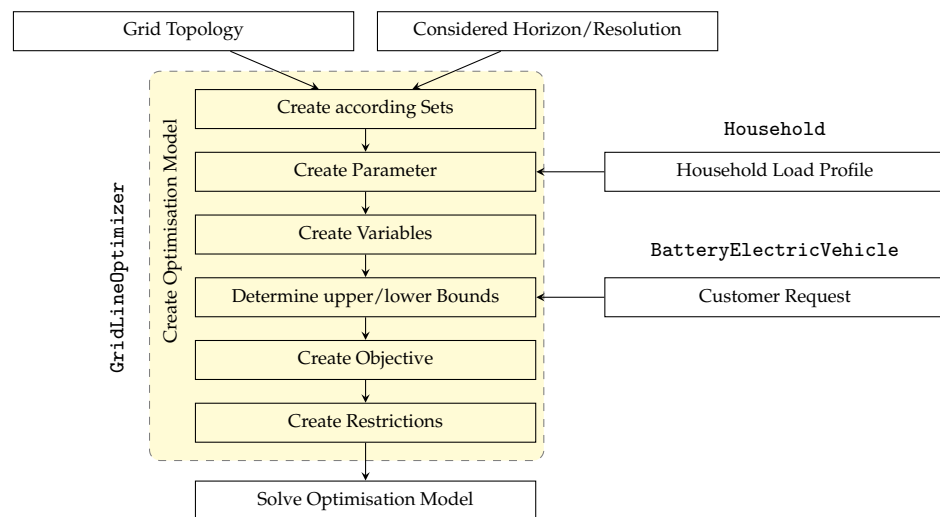

Figure 3. Data flow inside the grid line optimiser.

Currently, all the input parameters are obtained from scenarios prepared for simulation. In the future, the inputs for the grid topology will be derived from grid topology estimation, and household loads will be obtained from grid state estimation and real load profile data. Additionally, customers will be able to input their requests regarding SOC and finish time at the charging station via touch displays.

A generic grid line, as used for the optimisation, is shown in Figure 4. Charging stations and SMGs are attached to some grid nodes, such as n_2, while other grid nodes, such as n_1, do not have these attachments.
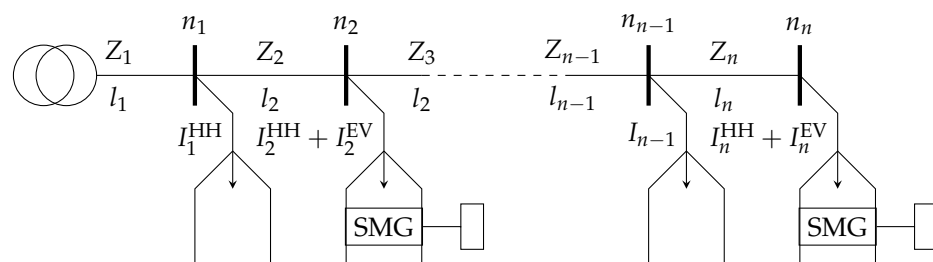

Figure 4. Generic grid line used for optimisation (SMG: smart meter gateway).

Within this example, the following assumptions are made:

- Only a single grid line is considered;
- House connection lines (and their impedances) are not considered;
- Node voltages are considered over time for the SOC calculation;
- Only the real part of line impedances is considered [22].

3.2. Linear Programming Design

In the following section, all the relevant equations and parameters of the optimisation are listed.

3.2.1. Sets

The following sets are used as indexing variables, parameters, and constraints:

- The set of time steps ($\mathcal{T} = \{1, \ldots, n\}$) in the considered horizon;
- The set of nodes ($\mathcal{N} = \{1, \ldots, n\}$) of the considered grid line;
- The set of nodes with a charging station attached ($\mathcal{N}_{\text{EV}} = \{1, \ldots, n\}$) in the considered grid line, where $\mathcal{N}_{\text{EV}} \subseteq \mathcal{N}$;
- The set of lines ($\mathcal{L} = \{1, \ldots, n\}$) of the considered grid line.

3.2.2. Variables

As variables serve the charging currents for each EV in the grid line at each time step:

$$I_{t,n}^{\text{EV}} \quad \forall t, n \in \mathcal{T} \times \mathcal{N}_{\text{EV}},$$

as well as their respective SOC:

$$SOC_{t,n} \quad \forall t, n \in \mathcal{T} \times \mathcal{N}_{\text{EV}}.$$

3.2.3. Parameters

Indexed parameters in the optimisation problem are:

- The impedances of the respective lines: $Z_l \quad \forall l \in \mathcal{L}$;
- The voltages at the respective nodes: $U_n \quad \forall n \in \mathcal{N}$;
- The currents of the respective household loads: $I_{t,n}^{\text{HH}} \quad \forall t, n \in \mathcal{T} \times \mathcal{N}$;
- The battery capacity of the respective EVs: $En \quad \forall n \in \mathcal{N}_{\text{EV}}$;
- The maximum permittable charging current of the respective EVs: $I_n^{\max} \quad \forall n \in \mathcal{N}_{\text{EV}}$;
- The maximum permittable current of the respective lines: $I_l^{\max} \quad \forall l \in \mathcal{L}$;
- The start SOCs of the respective EVs: $SOC_n^{\text{start}} \quad \forall n \in \mathcal{N}_{\text{EV}}$;
- The start time steps of the respective EVs: $t_n^{\text{start}} \quad \forall n \in \mathcal{N}_{\text{EV}}$;
- The requested target SOCs of the respective EVs: $SOC_n^{\text{target}} \quad \forall n \in \mathcal{N}_{\text{EV}}$;
- The requested target time steps of the respective EVs: $t_n^{\text{target}} \quad \forall n \in \mathcal{N}_{\text{EV}}$;
- The conceded target fulfillment of the respective EVs: $S_n \quad \forall n \in \mathcal{N}_{\text{EV}}$.

Singleton parameters include:

- The voltage on the transformer low-voltage side: U_0;
- The transformer nominal power: P_{Trafo};
- The minimum permittable node voltage: $U_{\min}$;
- The maximum permittable difference among EV charging currents: $\Delta I_{\max}$;
- The duration of a time step: Δt.

3.2.4. Objective Function

The charging current ($I_{t,n}^{\text{EV}}$) over all considered time steps and all the nodes with attached chargers should be maximised according to Equation (1).

$$\sum_{t \in \mathcal{T}} \left(\sum_{n \in \mathcal{N}_{\text{EV}}} I_{t,n}^{\text{EV}} \right). \tag{1}$$

3.2.5. Constraints

Equations (2)–(5) represent the most important constraints of the optimisation algorithm. Equation (2) prevents the voltage at the last node from dropping too low.

$$U_0 - \sum_{l \in \mathcal{L}} \left(Z_l \cdot \sum_{\substack{n \in \mathcal{N} \\ n \geq l}} \left(I_{t,n}^{\text{EV}} + I_{t,n}^{\text{HH}} \right) \right) \geq U_{\min} \quad \forall t \in \mathcal{T}. \tag{2}$$

Equation (3) ensures that the maximum permissible current ($I_{\text{max}} = P_{\text{Trafo}}/U_0$) is not exceeded.

$$\sum_{n \in \mathcal{N}} \left(I_{t,n}^{\text{EV}} + I_{t,n}^{\text{HH}} \right) \leq I_{\text{max}} \quad \forall t \in \mathcal{T}. \tag{3}$$

Equation (4) ensures energy conservation during charging.

$$SOC_{t,n} + \frac{I_{t,n}^{\text{EV}} \cdot U_n \cdot \Delta t}{E_n} \cdot 100\% = SOC_{t+1,n} \quad \forall t, n \in \mathcal{T} \times \mathcal{N}_{\text{EV}}. \tag{4}$$

Equation (5) ensures that the maximum current conductivity of the individual lines is not exceeded.

$$\sum_{\substack{n \in \mathcal{N} \\ n \geq l}} \left(I_{t,n}^{\text{EV}} + I_{t,n}^{\text{HH}} \right) \leq I_l^{\text{max}} \quad \forall t, l \in \mathcal{T} \times \mathcal{L}. \tag{5}$$

3.2.6. Additional Constraints for Fair Charging

Equations (6)–(11) describe further optional constraints that can be activated to ensure "fair" charging. Each of these additional constraints uses another definition of fairness.

Equation (6) ensures that every EV receives approximately equal charging power per time step. Therefore, a maximum tolerable difference (ΔI_{max}) in charging current is introduced.

$$I_{t,n}^{\text{EV}} - I_{t,m}^{\text{EV}} \leq \Delta I_{\text{max}} \quad \forall t, n, m \in \mathcal{T} \times \mathcal{N}_{\text{EV}}^2 \quad \text{with } n > m. \tag{6}$$

Equation (7) ensures that every EV received approximately the same target fulfillment (S_n), which may not deviate from one another by more than a maximum permittable difference ($\Delta S_{\text{max}} \in [0,1]$) in target fulfillment.

$$S_n - S_m \leq \Delta S_{\text{max}} \quad \forall n, m \in \mathcal{N}_{\text{EV}}^2 \quad \text{with } n > m. \tag{7}$$

Here, the target fulfillment (S_n) is defined according to Equation (8):

$$S_n = \frac{SOC_{t_{\text{end}},n} - SOC_n^{\text{start}}}{SOC_n^{\text{target}} - SOC_n^{\text{start}}} \tag{8}$$

where $SOC_{t_{\text{end}},n}$ is the final SOC actually reached by the EV at node n.

Equation (9) ensures that EVs that have started charging with a lower SOC receive more charging power than EVs that started charging with a higher SOC.

$$S_n \cdot SOC_n^{\text{start}} = S_m \cdot SOC_m^{\text{start}} \quad \forall n, m \in \mathcal{N}_{\text{EV}}^2 \quad \text{with } n > m. \tag{9}$$

Equation (10) ensures that EVs that have been waiting longer at the charger to be charged receive more charging power than EVs that have just arrived at the charger.

$$\sum_{t \in \mathcal{T}} \left(I_{t,n}^{\text{EV}} \right) \cdot \Delta \tau_n^2 = \sum_{t \in \mathcal{T}} \left(I_{t,n-1}^{\text{EV}} \right) \cdot \Delta \tau_{n-1}^2 \quad \forall n \in \mathcal{N}_{\text{EV}}. \tag{10}$$

where $\Delta \tau_n$ is the remaining energy required to charge in relation to the remaining time required to charge the EV at node n according to Equation (11):

$$\Delta \tau = \frac{t_n^{\text{target}} - t}{SOC_n^{\text{target}} - SOC_{t,n}} \tag{11}$$

where t_n^{target} is the time when EV at node n wants to be finished charging.

3.2.7. Bounds of the Variables

To ensure that the optimisation does not set charging current ($I_{t,n}^{\text{EV}} \neq 0$) when there is no EV charging at node n at time step t, the following Equation (12) determines the upper bounds ($\lceil I_{t,n}^{\text{EV}} \rceil$) of charging currents.

$$
\left\lceil I_{t,n}^{\text{EV}} \right\rceil = \begin{cases} 0 & \text{if } t < t_n^{\text{start}} \\ I_n^{\max} & \text{if } t_n^{\text{start}} \leq t < t_n^{\text{target}} \\ 0 & \text{if } t \geq t_n^{\text{target}} \end{cases} \qquad \forall n \in \mathcal{N}_{\text{EV}}. \tag{12}
$$

The lower bounds ($\lfloor I_{t,n}^{\text{EV}} \rfloor$) of charging currents are determined according to Equation (13).

$$
\left\lfloor I_{t,n}^{\text{EV}} \right\rfloor = 0 \quad \forall t, n \in \mathcal{T} \times \mathcal{N}_{\text{EV}}. \tag{13}
$$

For the SOC, the upper bounds ($\lceil SOC_{t,n} \rceil$) are chosen according to Equation (14).

$$
\lceil SOC_{t,n} \rceil = \begin{cases} SOC_n^{\text{start}} & \text{if } t = 0 \\ SOC_n^{\text{target}} & \text{if } t > 0 \end{cases} \qquad \forall n \in \mathcal{N}_{\text{EV}}. \tag{14}
$$

SOC lower bounds ($\lfloor SOC_{t,n} \rfloor$) are chosen according to Equation (15).

$$
\lfloor SOC_{t,n} \rfloor = SOC_n^{\text{start}} \quad \forall n \in \mathcal{N}_{\text{EV}}. \tag{15}
$$

It is important to note that the lower bounds for state of charge (SOC) are fixed at SOC_n^{start}. Setting SOC_n^{target} as the lower bound could cause the optimisation to fail if the target cannot be achieved. The formulation of the objective function in Equation (1) is sufficient for the optimiser to maximise charging currents and, hence, SOCs whenever possible. The upper bounds for SOC are set to SOC_n^{target} to prevent overcharging of EVs, which could result in other EVs being charged less.

3.3. Hardware Used for Optimisation

The optimisation algorithm was initially developed on a laptop, but in practical use, it needs to run on a Raspberry Pi 3. Therefore, a comparison of the performance characteristics of the laptop and the Raspberry Pi was conducted. In Table 2, a comparison of the most important characteristics of both devices is presented.

Table 2. Comparison of some characteristics of the used devices.

Device	Processor	RAM
Dell Inspiron 15	Intel Core i5 8250U; 1.80 GHz	8 GB
Raspberry Pi 3	ARMv8; 1.20 GHz	1 GB

4. Results

For the evaluation of the performance of the developed optimisation algorithm, various scenarios were modelled. Additionally, a comparison of computational time on a laptop and a Raspberry Pi is presented. A list of all the considered scenarios is provided in Table 3. In scenarios with control, there is also a P(U) control for comparison with the optimisation. The P(U) control regulates the charging power of the EVs based on the lowest node voltage across the grid, as described in [21]. In scenarios with "fairness", additional constraints are activated to ensure fair charging.

Table 3. Considered scenarios.

Scenario	Transformer Nominal Power [kVA]	Nodes	EVs	Control	"Fairness"
1	150	6	6	no	no
2	200	40	40	yes	no
3	250	40	40	yes	no
4	220	40	40	no	yes
5	15	6	2	no	yes

Unless explicitly stated otherwise, the following assumptions apply to all of the scenarios:

- The length of the individual lines is 20 m each;
- The specific impedance of the individual lines is $2 \times 10^{-4}\,\Omega\,\mathrm{m}^{-1}$ each;
- All the individual lines are expected to be able to conduct the same current;
- The battery capacity of the individual EVs is 50 kWh each;
- The nominal power of the individual charging stations is 11 kW (three-phase total) each;
- The household load profiles are taken from [23];
- The time resolution is 6 min;
- The considered time horizon is 24 h.

According to [24], the line lengths and impedances are typical values for a line of the type "NAYY 4 × 150 SE", which is commonly used in urban areas.

All the results can be validated using the software described in Appendix A. A detailed description of the customer requests assumed in each of the scenarios is provided in Appendix B.

These five scenarios were chosen to demonstrate how the optimisation algorithm handles specific situations. In Scenario 1, the goal is to show how the optimisation shifts the EV charging processes to prevent grid overload when there is a higher demand from uncontrollable household loads. In Scenario 2, the goal is to demonstrate that the optimisation is scalable to handle longer grid lines and situations in which all the EVs want to start charging at the same time. Scenario 3 aims to provide a comparison of the performance of the optimisation, P(U)-control, and uncontrolled charging over the course of one week. In Scenario 4, the goal is to compare the performance of different approaches for fair charging under extreme situations in which additional household loads congest the grid. Finally, in Scenario 5, the goal is to provide a detailed comparison of how different approaches for fair charging handle a situation that leads to unfairness.

4.1. Scenario 1: Demonstrate Load Shifting

The first scenario is designed to demonstrate load shifting in response to inflexible household loads. Since these household loads cannot be influenced by the optimiser, the optimiser shifts the EV loads to prevent grid overloading while still attempting to fulfill customer requests to the greatest extent possible. In this scenario, additional loads of 23.8 kW are added on top of each household profile from 11 a.m. to 7 p.m. to observe the reaction of the optimiser. The results of the optimisation for Scenario 1 are shown in Figure 5.

The transformer's nominal power is large enough to allow for multiple EVs to be charged simultaneously, for example, between 9 a.m. and 11 a.m. However, from 11 a.m. to 7 p.m., there is always only one EV charging at a time, and not even at nominal power. Only after 7 p.m. is one more charging possible at nominal power. Despite this, by the end of the day, all customer requests are fulfilled. It can be observed that between 11 a.m. and 7 p.m., the transformer load is at 100% due to the additional loads within each household. This is the reason why the optimiser shifts the EV charging outside of this time frame.
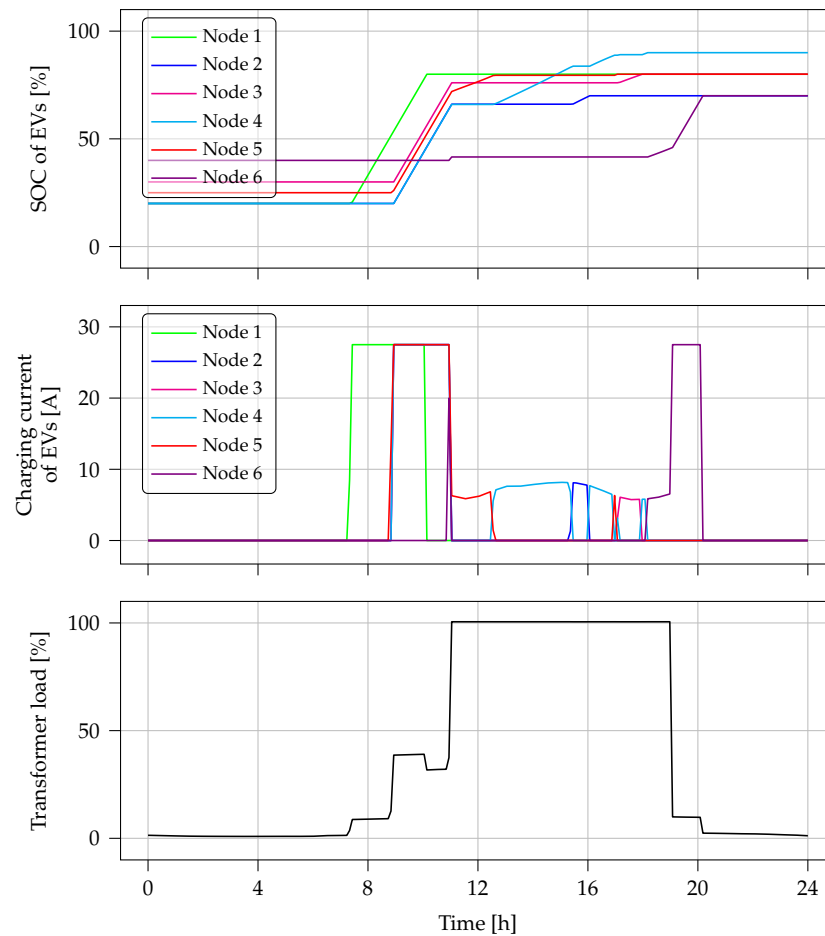
Figure 5. Results of optimisation for Scenario 1.

4.2. Scenario 2: Demonstrate Scalability

The second scenario aims to demonstrate the scalability of the algorithm and its ability to handle extreme situations. In this scenario, 40 nodes are considered, each with a charger and EVs connected. The EVs start with an SOC of 10% and wish to be charged to 100%. The start and target times are set at 12 a.m. and 6 p.m., respectively. No additional loads are added on top of the household loads, creating an extreme scenario in which all EVs start charging at the same time. The results are compared for different setups of the grid line. The first setup is optimised, the second setup is not optimised, and the third setup is P(U)-controlled. The resulting timelines for transformer load and the voltage at the last node are shown in Figure 6.

In the case with the optimiser, the node voltage always stays at 376 V. The transformer load remains at roughly 100%, never significantly exceeding this levle for many consecutive time steps. In the case of non-optimised charging, the transformer load exceeds 300% for nearly two hours, and the node voltage falls below 300 V. In the case of P(U) control, the transformer load also rises above 300%, and it takes around two hours for the transformer load to fall below 100%. Additionally, the node voltage falls below 300 V, and it takes some time to bring the voltage back above 376 V. The optimiser shifts EV charging to prevent any violation of grid overload criteria.

Without optimisation, a maximum of 5 EVs can start charging at the same time before the voltage drops below 376 V. However, with optimisation, all 40 EVs can start charging at the same time without overloading the grid. This corresponds to a 700% increase in the number of charged EVs.
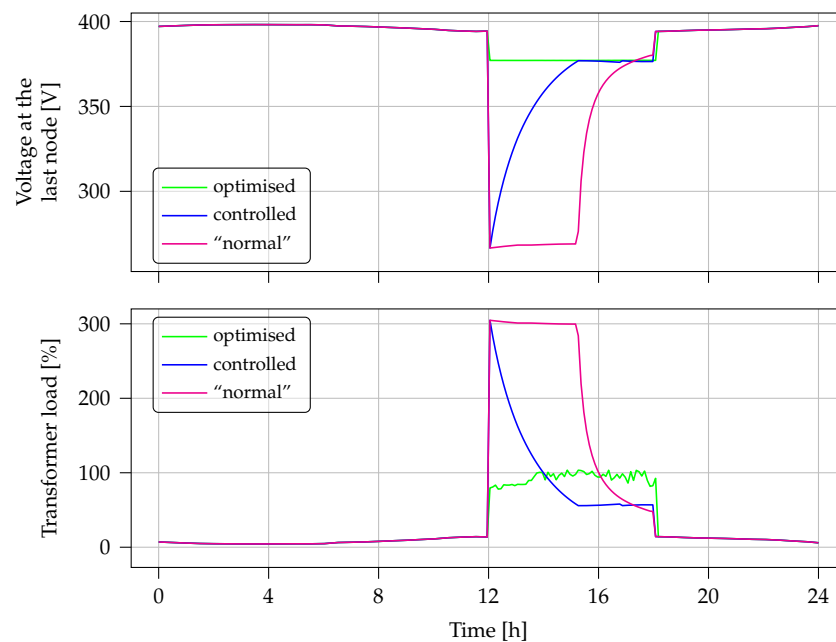
Figure 6. Results of optimisation for Scenario 2.

A box plot for the target fulfillment in each of the considered cases is shown in Figure 7. In the case of optimisation, almost all EVs are charged according to their requests, except for those at the last seven nodes, which are not charged at all. In the case of P(U) control, all EVs are charged to around 60% target fulfillment. In the "normal" case, all EVs are charged to 100% target fulfillment but at the cost of massive grid overload.
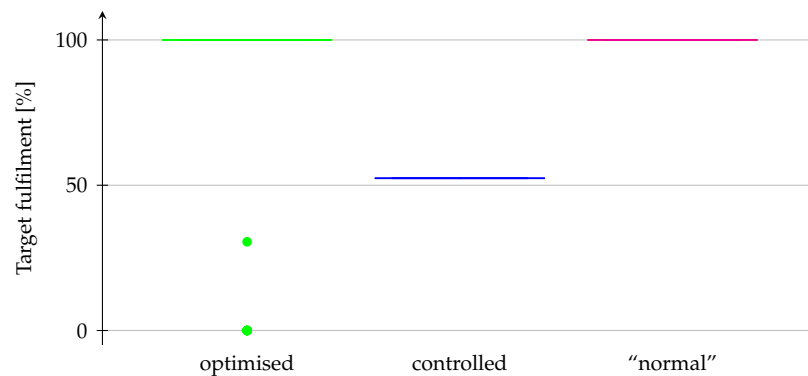

Figure 7. Target fulfillments for Scenario 2.

4.3. Scenario 3: Comparison over One Week

The third scenario involves a comparison of grid overload over the course of one week for different setups of the grid line. In the first setup, the optimizer is activated (optimized). In the second setup; the optimizer is deactivated ("normal"); and in the third setup, the optimizer is deactivated, but the P(U) control is activated (controlled). There are 40 nodes, with a charging station connected to each of them, but no additional loads are added to the households. Both the start/target SOC and start/target time are randomly generated. A total of seven days are simulated, and the transformer load and voltage at the last node are considered. The resulting timelines are shown in Figure 8, and the resulting duration curves are shown in Figure 9.
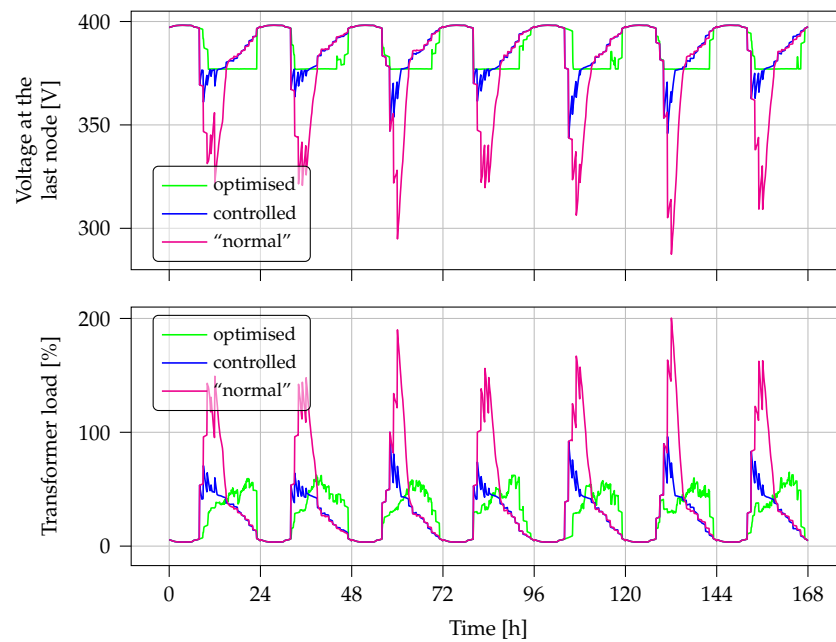
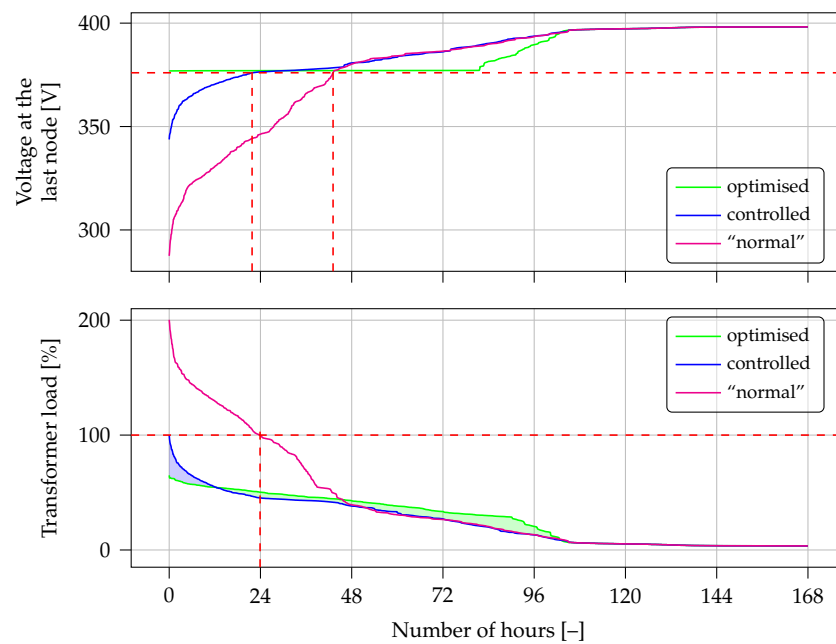**Figure 8.** Results of optimisation for Scenario 3.

Figure 9. Results of optimisation for Scenario 3—sorted timelines.

In the "normal" case, the transformer load exceeds 100% for almost 24 h within the week. However, with optimisation or control activated, the transformer load never exceeds 100%. Nevertheless, the optimiser keeps the transformer at a higher load for a longer time, resulting in more EVs being charged to higher SOCs, as is the case with P(U) control.

In the "normal" case, the node voltage drops below 376 V for almost 43 h in the week. With the control activated, there are only 22 h during which the voltage drops below 376 V. This is because the P(U) controller can only react once the voltage has dropped too low, and it takes some time to raise the voltage afterwards. Only the optimiser manages to keep the voltage above 376 V, thereby preventing the grid from being overloaded. However, the optimiser pushes the grid to its limits, maintaining the node voltage at around 376 V for roughly 80 h within the week, thereby maximising grid utilisation.

In Figure 10, the difference in transformer load between the setup with optimisation and the setup with control is shown. The green area represents times when the load on the transformer is higher for the optimisation case. The blue area represents times when the transformer load is higher in the case of P(U) control. The red dashed line represents the mean value. There are approximately 90 h within the week during which the transformer load is higher with the optimiser and almost 16 h during which the transformer load is higher with the controller. On average, the transformer load is 2.4% higher with the optimiser compared to the controller. With a transformer nominal power of 250 kVA, this translates to 6 kW. Over the course of a week with 168 h, this amounts to an additional 1000 kWh that can be charged. Considering an average battery capacity of 50 kWh, this corresponds to 20 additional complete EV cycles.
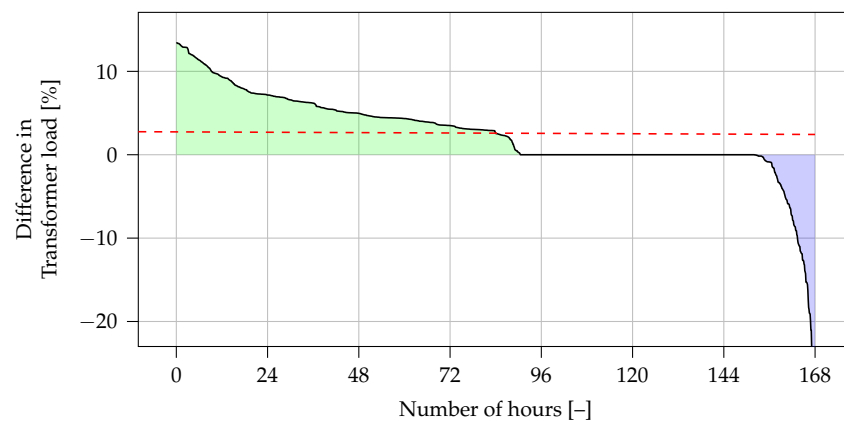

Figure 10. Results of optimisation for Scenario 3—difference between sorted timelines for transformer load in the case of optimisation and control.

The corresponding target fulfillments, calculated as mean values over the complete week, are shown in Figure 11. The optimiser not only charges more energy compared to P(U) control but also enables more homogeneous charging, resulting in smaller variance in target fulfillment. In the 'normal' case, some EVs are charged more than desired (target fulfillments > 100%) but at the cost of other EVs being charged less, resulting in grid overload each day.
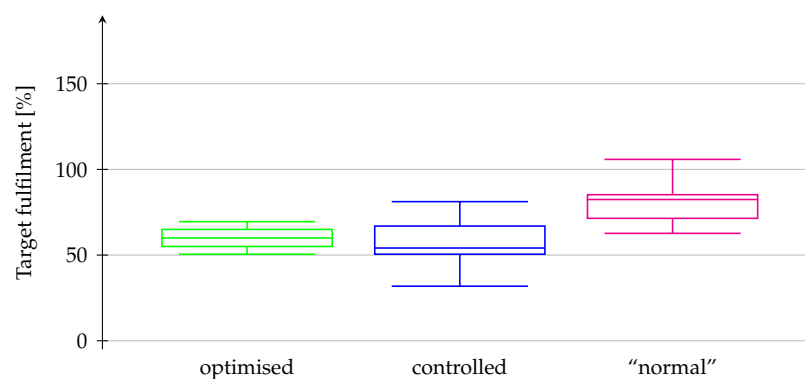

Figure 11. Mean target fulfillments for Scenario 3.

4.4. Scenario 4: Fair Charging under Extreme Conditions

The fourth scenario compares the performance of different strategies for fair charging by activating additional constraints from Equations (6), (7), (9), and (10) one at a time. There are 40 nodes, each with a charger attached, and the transformer nominal power is 220 kVA. The customer requests are randomly generated (but the same for each additional constraint). Additionally, from 11 a.m. to 4 p.m., there are additional loads of 1.8 kW added on top of each household. The results are shown in Figure 12.
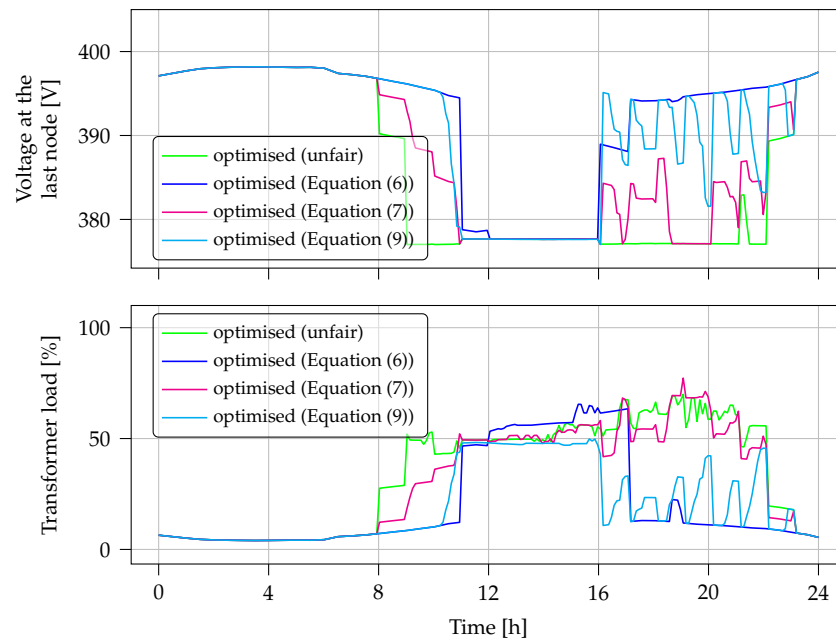
Figure 12. Results of optimisation for Scenario 4.

The results of optimisation with the constraint from Equation (10) are not shown here because the optimisation failed with this additional constraint activated because in the denominator of Equation (11), the difference between the desired SOC and the actual SOC is calculated. If an EV reaches the desired SOC, this leads to a division by zero.

In the time slot with the additional household loads, the optimisation manages to prevent grid overload, independent of the activated constraint. However, before and after that time slot, there are differences observed among the different additional constraints.

The achieved target fulfillments are shown in Figure 13. In the case of optimisation without additional constraints activated (unfair), most of the EVs are charged to 100% target fulfillment, except for a few EVs at the last nodes, which are not charged as much.

In the case with the constraint from Equation (6) additionally activated, most of the EVs end up with very low target fulfillment. This constraint formulation is too restrictive, as it does not allow for differences between the charging currents of the individual EVs, thereby preventing effective load shifting. As a result, the outcomes are unsatisfactory.

In the case with the constraint from Equation (7) additionally activated, different classes of target fulfillment can be observed. Within each class, all EVs reach exactly the same target fulfillment.
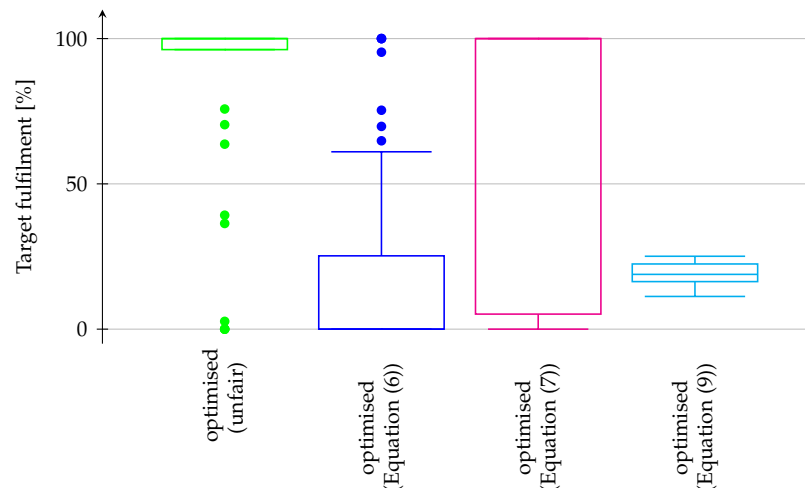

Figure 13. Mean target fulfilments for Scenario 4.

In the case with the constraint from Equation (9) additionally activated, the EVs also achieve low target fulfillments but with the lowest variance among them.

4.5. Scenario 5: Detailed Comparison of Fair Charging

The fifth scenario involves a detailed comparison of different constraints for fair charging. The additional constraints from Equations (6), (7), (9), and (10) are activated one at a time. The grid line consists of six nodes, with 2 EVs charging at nodes 1 and 6. The transformer has a nominal power of 15 kVA, which is not enough to charge both EVs simultaneously at their nominal power. Moreover, there are additional loads of 1.7 kW, each added to the household loads in a time window from 8 a.m. to 4 p.m.

The EV at node 1 starts charging at 12 a.m. with an SOC of 10%, while the EV at node 6 begins charging at 4 p.m. with an SOC of 30%. Both EVs aim to reach a 100% SOC by 9 p.m. However, the EV at node 1 is affected by the increased household load during a portion of its available charging time due to its charging time frame. The results of the optimisation for each of the additional constraints are presented in Figure 14.
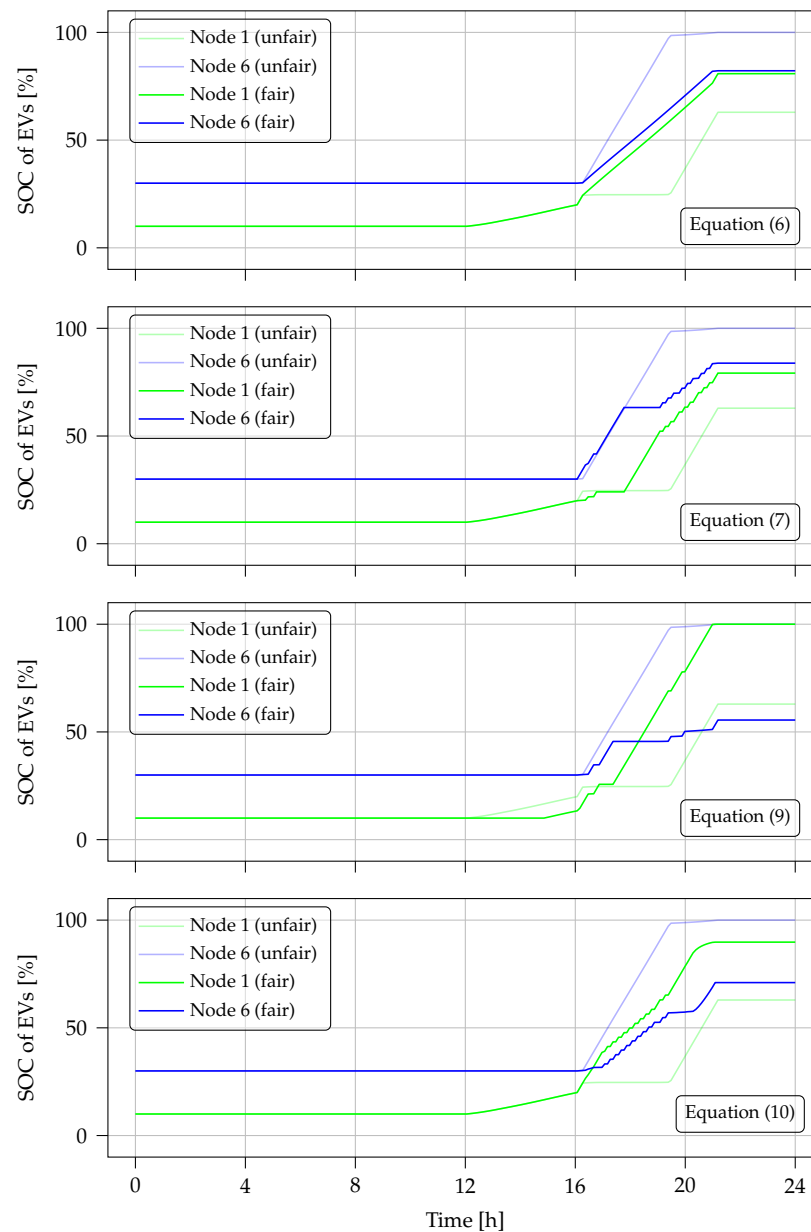

Figure 14. Results of optimisation for Scenario 5.

Here, the results of the optimisation without additional constraints are displayed with lower opacity to facilitate a direct comparison between fair and unfair optimisation. The additional restriction is listed in the bottom-right corner of the figure.

The EV at the first node, despite starting charging 4 h earlier, is charged less than the EV at the last node without additional constraints. This is because the increased household loads during the time window from 8 a.m. to 4 p.m. limit the available charging power. As a result, the EV at node 1 can only charge with a very low current from 12 p.m. to 4 p.m. Once the EV at node 6 starts charging at 4 p.m., the EV at node 1 is no longer allocated any charging current, even though it has been waiting at the charging station for a longer time. In contrast, the EV at node 6 receives the full charging power.

The constraint from Equation (6) requires that the difference between the charging currents of both EVs must be exactly 0 A ($\Delta I_{max} = 0$ A) for each time step. This is evident in the period from 4 p.m. to 9 p.m., during which the SOC of both EVs increases in parallel. However, there is a difference in the charging currents of the two EVs in the period from 12 p.m. to 4 p.m., as the additional household loads only allow for one additional charging process during that time.

The constraint from Equation (7) mandates that the difference between the target fulfillments of both EVs should be exactly 0% ($\Delta S_{max} = 0\%$). As a result, the optimiser alternately switches the charging processes on and off, leading to a fluctuating pattern in the SOCs of the EVs. However, both EVs ultimately reach the same target fulfillment, which may not necessarily result in the same SOC levels according to Equation (8).

The constraint from Equation (9) stipulates that the product of the SOC at the start of the charging process and the conceded target fulfillment should be the same for all EVs. This means that EVs starting with a lower SOC are given preference. As a result, in this case, the EV at node 1 is charged more than the EV at node 6, as it starts with a lower SOC.

The constraint from Equation (10) specifies that EVs that have been at the charging station for a longer duration are granted more charging power compared to those that have been there for shorter periods. As a result, the EV at node 1 is charged more than the EV at node 6. When the additional electrical load is removed at 4 p.m., the charging power of the EV at node 1 is increased. Initially, the EV at node 6 is granted a lower charging power. However, a "shaky" course of the SOCs can be seen from 5 to 7 p.m., indicating a similar phenomenon as with Equation (7).

4.6. Time Required to Solve the Optimisation Model

As described in Section 3.3, the optimisation algorithm was developed on a laptop. However, in practical use cases, the optimisation is intended to be run on Raspberry Pis. As shown in Table 2, the laptop outperforms the Raspberry Pi in terms of processing power and RAM. Therefore, the performance of the optimisation on both devices was compared using a test case scenario similar to Scenario 2. In this test case, the number of nodes is varied to simulate progressively more complex optimisation problems. Each optimisation problem is solved ten times to calculate the mean time required to solve the problem. The results achieved with both devices are presented in Table 4, where the time for creating and solving the problem is specified in each case.

Table 4. Comparison of time required to solve the optimisation problem.

Device			Number of EVs					
			10	20	30	40	50	60
Laptop	Create problem	[s]	0.29	0.61	0.84	1.1	1.51	1.91
	Solve problem	[s]	0.36	0.61	0.74	1.04	1.56	2.13
Raspberry Pi	Create problem	[s]	0.74	1.79	3.04	4.65	6.44	8.37
	Solve problem	[s]	0.91	1.91	3.25	5.2	8.41	16.02

A graphical representation of the results is shown in Figure 15. It can be observed that the time needed to solve the problem, especially on the Raspberry Pi, increases disproportionately for more complex optimisation problems. However, even on the Raspberry Pi, the most complicated scenario takes only about 25 s to solve.
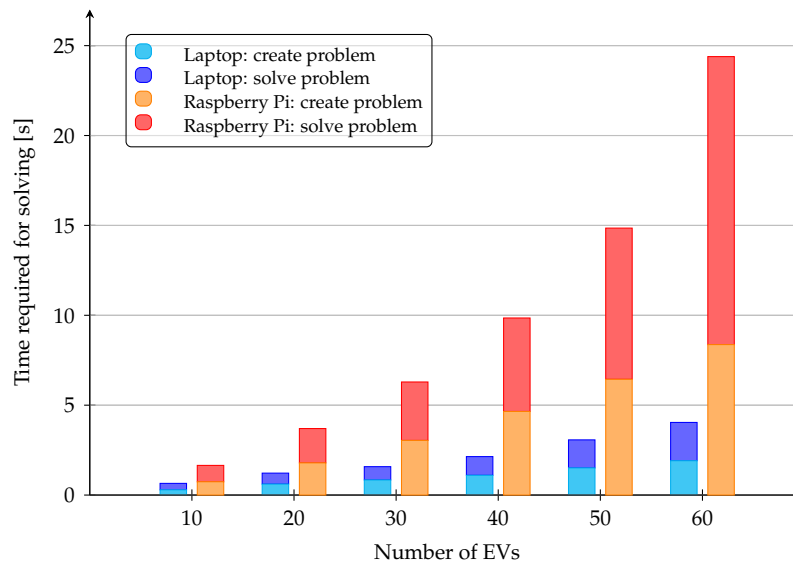

Figure 15. Comparison of required time to solve the problem on a laptop and on a Raspberry Pi.

This enables calling the optimisation each time new measurement data arrives from the smart meter gateway. Based on these new data, a corresponding optimisation problem will be created and solved, allowing the optimisation to react to sudden changes in input parameters. As a result, the solution of this new optimisation problem will be a new charging schedule that prevents grid overload for the updated conditions.

5. Discussion/Conclusions

The developed system enables optimal coordination of multiple EVs charging along a grid line. By using limited measurements, the grid topology and state can be reconstructed, which serves as input for the optimisation. Combined with other information such as household loads and customer requests, the optimisation determines an optimal charging schedule. This ensures that the grid is utilised to its limit but not beyond in order to charge as many EVs as possible. In cases in which it is not possible to fulfill all customer requests, the optimiser can still ensure fair charging.

To achieve fair charging, multiple approaches have been implemented, each with its own definition of fairness. All approaches are capable of enabling fair charging according to their respective definition. However, in extreme scenarios, some of these approaches may lead to unsatisfactory solutions due to their restrictive nature, excluding too many potential solutions. It should be noted that these extreme scenarios were intentionally chosen to test the optimisation algorithm, and in reality, it is unlikely that all EVs will start charging at exactly the same time.

Moreover, the proposed optimisation algorithm is scalable, as it can handle a varying number of nodes in the grid line and a varying number of attached charging stations. It can also accommodate different horizons and time resolutions. This means that the optimisation can be applied to grid lines of any length and with charging stations distributed arbitrarily.

The optimisation problem is formulated as a linear programming scenario and solved using the simplex algorithm, which ensures that the optimal solution can be obtained within a "reasonable" amount of time. This allows the optimisation to be executed regularly as new measurement data arrive, enabling timely reactions to unexpected changes in the grid load. A new optimisation problem incorporating the new data will be created and solved, resulting in an updated charging schedule for all the EVs.

However, the optimisation approach described in this paper is currently limited to single grid lines. In order to fully utilise the potential of the proposed system, future work should focus on extending the optimisation to accommodate arbitrary grid topologies. Additionally, while household loads are currently considered as standard load profiles, the capability to dynamically add loads on top of these profiles allows for simulation of more realistic scenarios. In the future, incorporating real measurement data from households will further enhance the accuracy and applicability of the optimisation approach.

As a next step, it would be interesting to explore the inclusion of controllable electric loads inside households in the optimisation. For instance, coordinating heat pumps with EV charging could help prevent grid overload. However, it is important to consider the impact on the optimisation time when adding more components. In particular, formulations that require binary variables may significantly increase the time needed to solve the optimisation problem. Careful consideration of the tradeoffs between model complexity and computational time will be crucial in future developments.

Author Contributions: Conceptualization, S.B., E.W. and I.S.; methodology, S.B. and A.U.; software, A.U. and C.H.; validation, A.U.; formal analysis, A.U.; investigation, A.U. and S.B.; resources, E.W. and S.B.; data curation, A.U.; writing—original draft preparation, A.U. and S.B.; writing—review and editing, S.B., I.S., E.W. and C.H.; visualization, A.U.; supervision, S.B., I.S. and E.W.; project administration, S.B., I.S. and E.W.; funding acquisition, I.S. All authors have read and agreed to the published version of the manuscript.

Data Availability Statement: Not applicable.

Abbreviations

The following abbreviations are used in this manuscript:

EV	Electric vehicle
GLO	Grid line optimiser
SMG	Smart meter gateway
GTE	Grid topology estimation
GSE	Grid state estimation
EMO	Simulation environment

Appendix A. Source Code of the Optimisation

The source code for the optimisation algorithm described in this paper can be found in the GitHub repository of the corresponding author: https://github.com/AndreGismo/Masterarbeit/tree/main/Code (accessed on 23 April 2023). The script `test_optimization.py` is the executable script. The scripts `optimization.py`, `household.py`, and `battery_electric_vehicle.py` hold the necessary definitions. The script `EMO.py` holds the code for the simulation environment (code is adapted from the author of [21]). The comments given in the source code are sufficient as a description. In case of further questions, the corresponding author may be contacted.

Appendix B. Detailed Customer Requests of the Scenarios

A detailed description of the customer requests assumed in each of the investigated scenarios presented in Section 4 is provided below. In case of many EVs, the customer requests are randomly generated using a fixed seed for reproducibility. In such cases, the needed parameters of the used equal distribution are given.

Table A1. Detailed customer requests in Scenario 1.

Node Nr.	Start SOC (%)	Target SOC (%)	Start Time (h)	Target Time (h)
1	20	80	2	10
2	20	70	2	16
3	30	80	2	18
4	20	90	2	18
5	25	80	2	17
6	40	70	2	20

Table A2. Detailed customer requests in Scenario 2.

Wish	Lower Bound	Mean	Upper Bound
Start SOC (%)	10	10	10
Target SOC (%)	100	100	100
Start time (h)	12	12	12
Target time (h)	18	18	18

Table A3. Detailed customer requests in Scenario 3.

Wish	Lower Bound	Mean	Upper Bound
Start SOC (%)	20	30	40
Target SOC (%)	60	80	100
Start time (h)	8	10	12
Target time (h)	15	19	23

Table A4. Detailed customer requests in Scenario 4.

Wish	Lower Bound	Mean	Upper Bound
Start SOC (%)	20	30	40
Target SOC (%)	60	80	100
Start time (h)	8	10	12
Target time (h)	15	19	23

Table A5. Detailed customer requests in Scenario 5.

Node Nr.	Start SOC (%)	Target SOC (%)	Start Time (h)	Target Time (h)
1	10	100	12	21
2	—	—	—	—
3	—	—	—	—
4	—	—	—	—
5	—	—	—	—
6	30	100	16	21

References

1. Ziele des Pariser Klimaabkommens Leicht Erklärt. Available online: https://www.lifeverde.de (accessed on 22 April 2022).
2. European Environment Agency. Available online: https://www.eea.europa.eu/ (accessed on 22 April 2022).
3. Statista. Available online: https://www.statista.com/statistics/1029872/newly-registered-plug-in-hybrid-and-battery-electric-cars-in-norway/ (accessed on 22 April 2022).
4. Chen, Y.H.; Lu, S.Y.; Chang, Y.R.; Lee, T.T.; Hu, M.C. Economic analysis and optimal energy management models for microgrid systems: A case study in Taiwan. *Appl. Energy* **2013**, *103*, 145–154. [CrossRef]
5. Zamarripa, M.; Vasquez, J.C.; Guerrero, J.M.; Graells, M. Detailed Operation Scheduling and Control for Renewable Energy Powered Microgrids. In *Computer Aided Chemical Engineering, Proceedings of the 21st European Symposium on Computer Aided Process Engineering, Athens, Greece, 29 May–1 June 2011*; Elsevier: Amsterdam, The Netherlands, 2011; Volume 29, pp. 1819–1823. [CrossRef]
6. Bhatt, P.K. Harmonics mitigated multi-objective energy optimization in PV integrated rural distribution network using modified TLBO algorithm. *Renew. Energy Focus* **2022**, *40*, 13–22. [CrossRef]

7. Rao, R.V.; Savsani, V.J.; Vakharia, D.P. Teaching–learning-based optimization: A novel method for constrained mechanical design optimization problems. *Comput.-Aided Des.* **2011**, *43*, 303–315. [CrossRef]

8. Christy, A.A.; Raj, P.A.D.V. Adaptive biogeography based predator–prey optimization technique for optimal power flow. *Int. J. Electr. Power Energy Syst.* **2014**, *62*, 344–352. [CrossRef]

9. Elattar, E.E.; ElSayed, S.K. Modified JAYA algorithm for optimal power flow incorporating renewable energy sources considering the cost, emission, power loss and voltage profile improvement. *Energy* **2019**, *178*, 598–609. [CrossRef]

10. Kanwar, N.; Gupta, N.; Niazi, K.R.; Swarnkar, A.; Bansal, R.C. Simultaneous allocation of distributed energy resource using improved particle swarm optimization. *Appl. Energy* **2017**, *185*, 1684–1693. . [CrossRef]

11. He, X.; Wang, W.; Jiang, J.; Xu, L. An Improved Artificial Bee Colony Algorithm and Its Application to Multi-Objective Optimal Power Flow. *Energies* **2015**, *8*, 2412–2437. [CrossRef]

12. Peças Lopes, J.A.; Soares, F.; Almeida, P. Integration of Electric Vehicles in the Electric Power System. *Proc. IEEE* **2011**, *99*, 168–183. [CrossRef]

13. Sortomme, E.; Hindi, M.M.; MacPherson, S.D.J.; Venkata, S.S. Coordinated Charging of Plug-In Hybrid Electric Vehicles to Minimize Distribution System Losses. *IEEE Trans. Smart Grid* **2011**, *2*, 198–205. [CrossRef]

14. Ahn, C.; Li, C.T.; Peng, H. Optimal decentralized charging control algorithm for electrified vehicles connected to smart grid. *J. Power Sources* **2011**, *196*, 10369–10379. . [CrossRef]

15. Cao, Y.; Kaiwartya, O.; Zhuang, Y.; Ahmad, N.; Sun, Y.; Lloret, J. A Decentralized Deadline-Driven Electric Vehicle Charging Recommendation. *IEEE Syst. J.* **2019**, *13*, 3410–3421. [CrossRef]

16. Liu, M.; Phanivong, P.K.; Shi, Y.; Callaway, D.S. Decentralized Charging Control of Electric Vehicles in Residential Distribution Networks. *IEEE Trans. Control Syst. Technol.* **2019**, *27*, 266–281. [CrossRef]

17. Al Zishan, A.; Moghimi Haji, M.; Ardakanian, O. Reputation-Based Fair Power Allocation to Plug-in Electric Vehicles in the Smart Grid. In Proceedings of the 2020 ACM/IEEE 11th International Conference on Cyber-Physical Systems (ICCPS), Sydney, NSW, Australia, 21–25 April 2020; pp. 63–74. . [CrossRef]

18. VDE. Erzeugungsanlagen am Niederspannungsnetz (VDE-AR-N 4105). 2018. Available online: https://www.vde.com/de/fnn/themen/tar/tar-niederspannung/erzeugungsanlagen-am-niederspannungsnetz-vde-ar-n-4105-2018 (accessed on 28 February 2023).

19. Bynum, M.L.; Hackebeil, G.A.; Hart, W.E.; Laird, C.D.; Nicholson, B.L.; Siirola, J.D.; Watson, J.P.; Woodruff, D.L. *Pyomo—Optimization Modeling in Python*, 3rd ed.; Springer Science & Business Media: Berlin/Heidelberg, Germany, 2021; Volume 67.

20. GLPK—GNU Project—Free Software Foundation. Available online: https://www.gnu.org/software/glpk/?msclkid=00d8d8cdacc611ec96ac382d182117e2 (accessed on 26 March 2022).

21. Hotz, C.; Baum, S.; Waffenschmidt, E.; Stadler, I. Estimating topologies of low voltage grids from electric vehicle charging point measurement data. In Proceedings of the CIRED Porto Workshop 2022: E-Mobility and Power Distribution Systems, Porto, Portugal, 2–3 June 2022; pp. 804–808. . [CrossRef]

22. Waffenschmidt, E.; Hotz, C.; Baum, S.; Stadler, I. Swarm Grids—Verteilte Stromnetzsteuerung für verteilte erneuerbare Energieerzeugung. In Proceedings of the Tagung Zukünftige Stromnetze, Online, 26–27 January 2022.

23. N-ERGIE-Netz. Available online: https://www.n-ergienetz.de/public/remotemedien/media/nng/produkte_und_dienstleistungen_2/30_netznutzung/N_Standardlastprofile_Strom_2020_Regelzone_TenneT.xlsx (accessed on 25 May 2021).

24. Kerber, G. Aufnahmefähigkeit von Niederspannungsverteilnetzen für die Einspeisung aus Photovoltaikkleinanlagen. Ph.D. Thesis, Technische Universtität München, Munich, Germany, 2011.